Construction and Building Materials 391 (2023) 131878

Contents lists available at ScienceDirect

Construction and Building Materials

journal homepage: www.elsevier.com/locate/conbuildmat

Feasibility of incorporating SO_4^{2-}-ions in zeolite-like matrices based on alkaline aluminosilicate binders

Pavel Krivenko [a], Igor Rudenko [a], Oleksandr Konstantynovskyi [a,*], Danutė Vaičiukynienė [b]

[a] Scientific Research Institute for Binders and Materials, Kyiv National University of Construction and Architecture, Povitroflotskyi Prospect 31, Kyiv 03037, Ukraine
[b] Faculty of Civil Engineering and Architecture, Kaunas University of Technology, Studentu St. 48, LT-51367 Kaunas, Lithuania

ARTICLE INFO

Keywords:
Alkaline aluminosilicate binder
Coating
Concrete deterioration
Sulfate environment
Zeolite-like matrix
Water resistance

ABSTRACT

Factors determining minimization of the influence of sulfate environments on concrete and risk of corrosion of embedded steel reinforcement have been analyzed. Coatings based on alkaline aluminosilicate binders were proposed to prevent transport of the sulfate ions into concrete. The formation of water resistant zeolite-like matrices on the alkaline aluminosilicate binder of the Na_2O-K_2O-Al_2O_3-SiO_2-H_2O system at 20 ± 2 °C can be provided by the use of calcium-containing modifying additives. Optimized molar ratios between oxides of binder constituent were SiO_2/Al_2O_3 = 4–5 and $K_2O/(Na_2O + K_2O)$ = 0.15–0.30. The results of the study show that the speed of incorporating sulfate ions in cement matrix of binder from the sulfate environment is dependent upon a cation and ranks as follows: $(NH_4)_2SO_4 > MgSO_4 > Na_2SO_4 > CaSO_4$. Complete protection of concrete against the penetration of sulfates can be reached when the developed coating is applied in a thickness of 3 mm.

1. Introduction

Choice of measures on how to enhance durability of reinforced concrete structures is one of the main challenges of building industry [1,2]. One of the factors determining durability of such structures is service conditions, especially under attacks of aggressive environments [3]. Currently, according to statistics, 75 % of building structures, such as those of chemical, energy generating industries [4], marine infrastructure [5], basements of bridges, tunnels [6], and systems of sewage water removal of megapolises [7] are exposed to aggressive environments.

Sulfate environments are the most widely met aggressive environments associated with durability of concrete and reinforced concrete structures [8]. This is attributed to the presence of sulfates in practically all types of waters [9].

Portland cement concrete exposed to highly aggressive sulfate environments undergoes degradation. Under external action of sulfates, the sulfate ions start to penetrate into pores of a cement stone. The formation of gypsum dihydrate $CaSO_4{\cdot}2H_2O$ and ettringite $3CaO{\bullet}Al_2O_3{\bullet}3CaSO_4{\cdot}32H_2O$ is due to interaction of these ions with portlandite $Ca(OH)_2$ and calcium aluminate hydrate [10]. These processes lead the internal stresses due to changes in the volume of crystalline phases within a restricted pore space. The internal stresses in the cement matrix result one's degradation [11]. The formation, in the presence of soluble carbonates, of thaumasite $CaO{\bullet}SiO_2{\bullet}CaCO_3{\bullet}CaSO_4{\cdot}15H_2O$ also affects negatively a microstructure and results in strength decline [12].

A negative influence of aggressive environments is associated not only with a risk of degradation of a concrete structure, but with risk of corrosion of steel reinforcement. The sulfate ions, though do not lead to a direct depassivation of steel, however, they promote the formation of H_2S and serve as catalysts of oxidation process (carbonation) of the resulted hydration products [13]. This is accompanied by the lowering of a pH-value of the pore liquid. pH-value is considered as a main factor determining a resistance of the passivating film that occurs on the surface of steel [14].

The processes of sulfate corrosion and their rates are determined by a concentration of the sulfate ions, chemical and mineralogical composition of a binder [15], and a type of cation of sulfate salt [16]. Sulfates of calcium [17], sodium, and magnesium are met the most frequently in underground, sewage waters, sea water and other waters [18]. A majority of structures of mining industry, nuclear energy and chemical industries suffer from deterioration initiated by aggressive substances, such as, for example, sulfate of ammonium [19].

Not depending upon a cation type, sulfates in the process of interaction with the hydration products of a cement stone are capable to

* Corresponding author.
E-mail address: alexandrkp@gmail.com (O. Konstantynovskyi).

https://doi.org/10.1016/j.conbuildmat.2023.131878
Received 1 August 2022; Received in revised form 11 April 2023; Accepted 17 May 2023

form, chiefly, such sulfate-containing phases as gypsum dihydrate, ettringite, thaumasite, which affect the processes of concrete degradation [20]. A solution of magnesium sulfate leads to additional formation, side by side with the above mentioned phases, of brucite $Mg(OH)_2$, which determines the occurrence of internal stresses and deformations [21].

The deterioration rate on concrete for sulfate salts ranks as follows: $(NH_4)_2SO_4 > MgSO_4 > Na_2SO_4 > CaSO_4$. This can be attributed to a solubility of the corresponding salts, chemical activity, size of cations and their ability to interact with amorphous phases and crystalline hydration products of the resulted cement stone [22].

Nowadays, there exist a number of measures to protect concrete against action of aggressive sulfate environments. Portland cement concretes with low penetration and high corrosion resistance, are well-known to be added with slags, fly ashes, and microsilica [23,24]. These materials are in compliance with current trends of building industry development [25,26].

One of the measures to prevent transport of the sulfate ions into concrete body is to produce a concrete with the lower porosity. Densification of concrete can be achieved due to the use of surface active substances with a water-reducing effect [13]. However, their compatibility with a cement still to be under a question. The water reducing surface active substances based on polyesters are considered as the most effective substances for Portland cement-based concretes [27,28]. However, with the higher contents of slag component of the cement composition the effect of these surface active substances tends to reduce [29] and in case of the alkali-activated slag cements can even approach zero [30]. The principles laid down in a proper choice of surface active substances and complex additives based on them for the alkali-activated slag cement concretes are aimed to provide a plasticizing effect [31], to reduce shrinkage deformations [32,33,34], to enhance crack resistance [35], to add expansive effect [36,37].

Protective coatings are used to protect already built structures from penetration of aggressive ions into a concrete and provide, thus, a passive condition of steel reinforcement [13]. The principles laid down in a choice of appropriate protection for concrete surface in order to prevent its degradation under action of aggressive environments, can be divided into four categories: surface coating [38]; pore blocking surface treatment [39,40]; hydrophobic impregnation [41], multifunctional (combined) surface treatment [42,43].

Depending upon a chemical nature, protective coatings can be organic [44] and inorganic ones [45]. Organic coatings are effective for protection of reinforced concrete structures intended for the work in aggressive environments [46]. However, the durability of organic coatings applied in a thin layer (thickness – 100–400 μm) under the combined action of ultraviolet radiation and aggressive environments is still under question [47].

Among various inorganic protective coatings, Portland cement-based coatings, modified by polymer admixtures (acrylic, epoxy or polyurethane ones) are very popular products [48]. They have, compared to organic coatings, high performance properties and high resistance against ultraviolet radiation, however, they are very expensive products [49].

Inorganic coatings based on the alkaline aluminosilicate binders (called also geopolymers) for a concrete protection are well known [50]. These coatings can be considered as a vital alternative to organic ones thanks to their high sulfate- and chloride resistance, resistance in organic and inorganic acids as well [51,52]. The coatings based on the alkaline aluminosilicate binders are known for their low water penetration [53], high freeze/thaw resistance [54], as well as high adhesion to different substrates, such as concrete [55,56], steel [57], wood [58,59], ceramics [60]. The enhanced durability and high protective properties in case of sulfate environments can be attributed to the formation in the reaction products of analogs to natural minerals: zeolites and feldspathoids [61]. Zeolites are themselves aluminosilicate hydrates with a Si-O-Al framework (consists, chiefly, of silica and alumina tetrahedra linked by shared oxygen atoms), well-defined channels and chambers filled by ions and molecules of water [62]. High adsorption and ion exchange capacity of the zeolite-like phases determine a direction of the best intended use of the alkaline aluminosilicate binders and materials based on them: water purification [63], immobilization of heavy metals and radionuclides [64,65], in process of CO_2 - adsorption [66], etc. An adsorption mechanism, which is accompanied by exchange of the ions from the framework and external ions, consists of two processes: physical adsorption and chemisorption [62]. A physical adsorption is associated with the intermolecular forces of Van der Waals as distance-dependent interactions between atoms or molecules, electrostatics and other types of interactions [67]. The chemisorption initiates the formation and break of intermolecular chemical bonds and, on the contrary to the process of physical adsorption, leads to the formation of modified zeolite-like minerals as a result of incorporation of these ions. As a result, other properties can be obtained [62,67].

A prevalence of this or that mechanism of adsorption is predetermined by a nature of ion and structure of zeolite. The formation of zeolite, in its turn, is determined by a number of factors, such as type of precursor, type of alkaline component, curing regimes, etc.

For example, immobilization of the chlorine (Cl^-) ions using the alkaline aluminosilicate binders based on metakaolin and fly ash can be provided as a result of both processes of adsorption mechanism: physical adsorption and chemisorption, and finally chloride-bearing zeolites (e.g., chabazite-Cl) are formed [68].

This adsorption mechanism is explored in immobilization of radioactive ions, for example, cesium (Cs^+) and strontium (Sr^{2+}), in the zeolite-like phases like $Na_{0.9}K_{0.1}GP$, analcime ($NaAlSi_2O_6{\cdot}H_2O$) and zeolite-P ($Na_{3.6}Al_{3.6}Si_{12.4}O_{32}{\cdot}14H_2O$) [69]. The formation of these minerals is reached by optimization of both a Na/K molar ratio in a precursor and choice of curing parameters.

According to [70], the sulfate ions can be incorporated in the zeolites $Na_8[AlSiO_4]_6(OH)_2{\cdot}2H_2O$ of the CAN-type, which are formed in the process of hydration of the alkaline aluminosilicate binders based on blends of sulfate-bearing kaolinitic clay and sludge of sandstone rock as a precursor after hydrothermal curing.

These data can predict an efficiency of the coatings based on the alkaline aluminosilicate binders for protection against aggressive sulfate environments. Such efficiency is reached by incorporating the sulfate ions and the following cations, these are: sodium, magnesium, ammonium, which also initiate degradation of concrete, in the zeolite-like phases as a result of chemisorption. The sulfate ion and the Si/Al molar ratio in a precursor affect essentially the ion exchange process. So, the exchange process of hydroxyl and sulfate ions prevail in the solution of sodium sulfate, whereas the exchange process of sodium and magnesium ions tends to become more intensive in the solution of magnesium sulfate. Also, the Si/Al molar ratio affects essentially corrosion resistance of the resulted hardened alkali activated material in the solution of magnesium sulfate, whereas in the solution of sodium sulfate its effect is not so essential [71].

A main challenge with regard to the use of protective coatings based on the alkaline aluminosilicate binders is a necessity to provide elevated temperatures (>40 °C) for their hardening. Such conditions ensure to obtain a water resistant zeolite-like minerals in the phase composition of hardened alkali-activated material [72]. Also, still actual is a question about conditions for a synthesis of the zeolite-like phases, which would allow for to obtain the formation of a hardened alkali activated material at 20 ± 2 °C.

Ratios of oxides in the alkaline aluminosilicate binder predetermine a phase composition and properties of the resulted hardened alkali-activated material [73]. The corrosion resistant zeolite-like phases are formed when the SiO_2/Al_2O_3 molar ratios are within the range of 2–7 and $(Na_2O + K_2O)/Al_2O_3 = 1$. Thus, optimization of the ratios of the above oxides can promote the formation of the zeolite-like minerals in a phase composition of hardened alkali-activated material at 20 ± 2 °C.

Another factor, which can accelerate the synthesis of the mentioned

Table 1
Chemical composition of binder components (% by mass).

Component	CaO	SiO_2	Al_2O_3	Fe_2O_3	MgO	SO_3	TiO_2	$K_2O + N_2O$	LOI
Metakaolin	0.27	54.08	43.61	0.77	0.52	–	–	0.25	0.50
Tripoli powder	0.83	85.59	6.20	3.15	0.95	0.39	2.03	0.67	0.19
Slaked lime	96.30	–	–	–	3.00	–	–	–	0.70
Portland cement	65.00	21.00	5.60	4.80	2.50	0.70	–	0.15	0.25
GBFS	46.99	39.93	7.22	–	5.49	–	0.37	–	–
High alumina cement	40.10	5.50	41.50	11.40	1.20	–	–	–	0.30
Fly ash	2.94	52.38	25.25	13.62	2.04	0.41	0.97	0.71	1.69

zeolite-like phases in the hardened alkali-activated material at normal temperatures, is the use of calcium-containing modifying additives. As reported in [74], the abovementioned modifying additives are the most effective for structure formation intensification in providing water resistance of the hardened alkali-activated material.

With consideration of the above information, **the aim** of the research is to study prevention of corrosion of reinforced concrete structures under attacks of sulfate environments in case of using the proposed coating based on the alkaline aluminosilicate binder of the Na_2O-K_2O-Al_2O_3-SiO_2-H_2O system, which (the binder) is capable to form the zeolite-like matrices and to bind sulfate ions. Metakaolin and tripoli powder (fine powdered porous sedimentary rocks, amorphous silica) were used as aluminosilicate components of the alkaline aluminosilicate binder (further, the binder). Sodium water glass and a solution of potassium hydroxide were used as alkali activators of the binder. Specified raw materials were chosen for ensuring the oxide composition ($Na_2O + K_2O$)•Al_2O_3•mSiO_2·nH_2O of the binder. The ratio between components, as well as the values of m and n, were calculated for each of the specified composition. The coatings were prepared by mixing the binder components, fillers, chemical additives, and reinforcing agents. The efficiency of the proposed protective coating was evaluated by such figures: freeze/thaw resistance of the coated concrete specimens, the strength of adhesion of the coating to a concrete substrate, water impermeability of the coated concrete, coefficient of corrosion resistance of the coated concrete and depth of penetration of the sulfate ions from aggressive environments into the underlying concrete structure.

2. Materials and methods

2.1. Materials

A binder was used in the design of the coatings.
The major components of the binder (Table 1) were:

- metakaolin ARGICAL-M 1200S (Imerys Minerals Refractory, France) (acc. to CAS 15123-81-6), pozzolanic reactivity = 1250 mg $Ca(OH)_2$/g (Chapelle test), specific surface area = 800 m^2/kg (by Blaine), specific gravity = 2.4 g/cm^3, particle size = 1.5 μm, purity 93.8 %;
- sodium water glass (TM Klebrig, Ukraine) (acc. to CAS 1344-09-8), silicate modulus Ms = 2.8, density = 1430 кg/m^3, concentration = 574.7 g/L, purity 99.0 %.

In order to adjust the composition of the binder with regard to contents of main oxides the following components were used:

- tripoli powder (PJSC «Kirovograd mechanical plant», Ukraine) (acc. to CAS 1317-95-9), specific surface area = 800 m^2/kg (by Blaine), bulk density = 2300 kg/m^3, porosity ≥ 70 %, purity 98.0 %;
- solution of potassium hydroxide KOH (TM Klebrig, Ukraine) (acc. to CAS 1310-58-3), density = 1430 кg/m^3, concentration = 615.8 g/L, purity 95.0 %.

Used as calcium-containing modifying additives to promote condensation of sodium water glass at normal temperatures were:

- slaked lime (TM Klebrig, Ukraine) (acc.to CAS 1305-62-0), specific surface area = 400 m^2/kg (by Blaine), purity 95.0 %;
- Portland cement CEM I 42,5 (PC «Ivano-Frankivskcement») (acc. to EN 197-1), specific surface area = 320 m^2/kg (by Blaine);
- high alumina cement Istra 40 (Calucem, Croatia) (acc. to EN 14647), specific surface area = 350 m^2/kg (by Blaine);
- granulated blast furnace slag (further, GBFS) (JSC «Kamet-steel», Ukraine) (acc.to DSTU B V.2.7-302), basicity modulus of 1.11, glass phase content of 84 % by mass, specific surface area = 420 m^2/kg (by Blaine).

A chemical composition of binder components is given in Table 1.

A liquid constituent of binder was prepared by mixing sodium water glass and water solution of KOH. A dry constituent of binder was prepared by mixing metakaolin, tripoli powder, and calcium-containing modifying additives. The binder was prepared by mixing an alkaline solution with a dry constituent in a Hobart mixer. The ratio between components, as well as the values of m and n, were calculated for ensuring the specified oxide composition ($Na_2O + K_2O$)•Al_2O_3•mSiO_2·nH_2O of the binder.

The binder-based coating mixtures were prepared by mixing an alkaline solution with the dry constituent of the binder, fillers, chemical additives, and reinforcing agent. The mixing was realized in a Hobart mixer.

Used as fillers were:

- fly ash (LLC «Ultra-trade», Ukraine) (acc. to DSTU B V.2.7–205), fr. ≤ 0.16 mm, bulk density = 1150 kg/m^3, specific surface area = 300 m^2/kg (by Blaine);
- quartz sand of two fractions: ≤0.315 mm and 0.315–0.63 mm.

A complex additive, consisting of Na_3PO_4·12H_2O (acc. to CAS 7601-54-9) (TM Klebrig, Ukraine, purity = 98 %) and sodium gluconate (acc. to CAS 527-07-1) (TM Klebrig, Ukraine, purity = 99 %), was used to provide a required consistency and workability retention. Carboxymethyl cellulose ("Gabrosa HV" AkzoNobel, Netherlands) was used to add a water-retaining capacity to the binder-based coating mixture.

Basalt mica fr. ≤ 1.0 mm (Ltd «Basalt Fiber & Composite Materials Technology Development», China) (bulk density = 25 kg/m^3, specific gravity = 1.8 g/cm^3) was used as a reinforcing agent to increase crack resistance and physico-mechanical characteristics of the coatings.

2.2. Testing methods

The values of viscosity of the binder mixtures and consistency of the binder-based coating mixtures were measured using a viscometer acc.to Suttard.

After preparation, 40x40x40 mm specimens of the binder and binder-based coatings were allowed to harden at t = 20 ± 2 °C and RH = 95 ± 5 % for 1 day in moulds, then were taken from the moulds and stored for the further 27 days. The values of compressive and flexural strength were determined in accordance with the EN 196-1 standard.

A coefficient of water resistance (K_w) of the binder was determined at specified ages of 2, 7, and 28 days. After preparation the specimens were kept in moulds for 1 day, then until specified ages in water. A value of

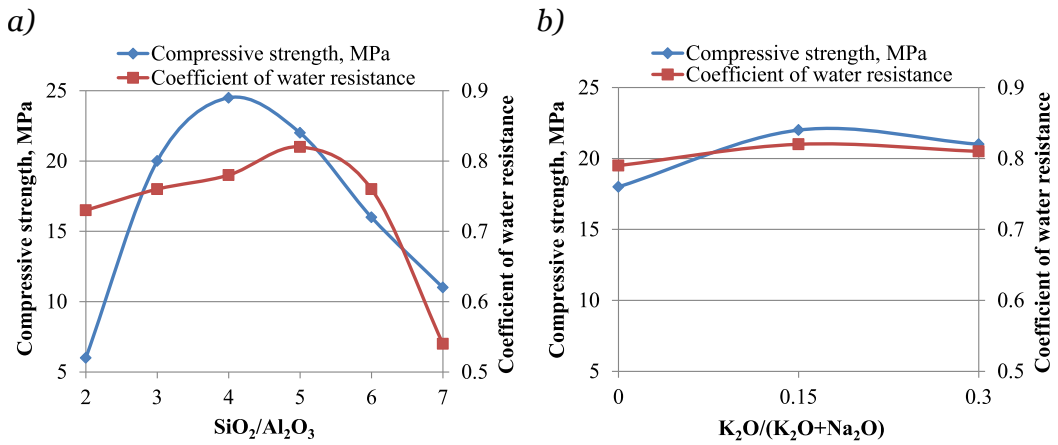

Fig. 1. The influence of varying SiO_2/Al_2O_3 molar ratio at $K_2O/(K_2O + Na_2O) = 0.15$ (a) and $K_2O/(K_2O + Na_2O)$ molar ratio at $SiO_2/Al_2O_3 = 5.00$ (b) on strength and water resistance of the hardened binder after hardening for 28 days at t = 20 ± 2 °C and RH = 95 ± 5 %.

the coefficient was calculated as a ratio of the values of compressive strength of the specimens at specified ages to those of the specimens that hardened until specified ages under normal conditions. It is accepted that a material is classified as a water resistant material, when $K_w \geq 0.8$.

Freeze/thaw resistance of the coated C30/35 concrete specimens was studied in accordance with the national standard of Ukraine DSTU B V.2.6-181. The thickness of the coating of 2 mm. According to this accelerated method, the 100 mm cube specimens after 28 days of storage at t = 20 ± 2 °C and RH = 95 ± 5 % were saturated with 5 % solution of NaCl at t = 18 ± 2 °C for 48 hr and after that were subjected to freezing at t = −50 ± 5 °C. Thawing was done in 5 % solution of NaCl. A grade of concrete in freeze/thaw resistance (F) is a number of alternate freezing and thawing at which a mean adhesion of the coating to a concrete substrate decreased by no >35 %. The freeze/thaw resistance of the coated concrete was assessed by the correspondence between permissible number of freezing/thawing cycles by the accelerated method and by the first method prescribed in the national standard of Ukraine DSTU B V.2.7-48.

The strength of adhesion of the coating to a concrete substrate was determined in accordance with the national standard of Ukraine DSTU B V.2.6-181 by measuring a perpendicular tensile force, required for separation of the coating from the concrete substrate with the help of a bonded metal stamp and dynamometer.

Water impermeability (W) of the coated concrete was evaluated in accordance with the national standard of Ukraine DSTU B V.2.6-181. The thickness of the protective coating of 2 mm. The coated cylinder concrete specimens of Ø150 × 50 mm that hardened at t = 20 ± 2 °C and RH = 95 ± 5 % were subjected at age of 28 days to action of water under pressure. The pressure was increased in steps, each step being −0.2 MPa. Time of storage at each step was 6 hr. Grade of concrete in water impermeability is a maximal pressure of water (MPa•10^{-1}), at which the water penetration through the specimen was not observed.

Efficiency of protective properties of the coatings was evaluated by a coefficient of corrosion resistance of the coated concrete, and depth of penetration of the sulfate ions from aggressive environments into the underlaying concrete structure was tested on the coated 40x40x160 mm fine aggregate concrete specimens. The coatings were applied on side surfaces of the hardened concrete specimens in three thicknesses (1, 2, 3 mm) and stored for 28 days at t = 20 ± 2 °C and RH = 60 ± 5 %. Afterwards, the uncoated specimens (reference specimens) were placed vertically in water and the coated specimens–into solutions of sodium, magnesium and ammonium sulfates. The concentration of the sulfate ions was 30000 mg/L. Corrosion resistance of the coated concrete specimens was evaluated by a coefficient of corrosion resistance (K_{cr}), which is a ratio of flexural strength of the coated concrete specimens and stored in sulfate environments, to those of the reference specimens stored in water. The thickness of the coating of 1 mm. A concrete is classified as a not corrosion resistant ($K_{cr} < 0.3$), lowly corrosion resistant ($0.3 < K_{cr} < 0.5$), corrosion resistant ($0.5 < K_{cr} < 0.8$), and highly corrosion resistant ($K_{cr} > 0.8$) concrete.

After 360 days of storage in the aggressive environments the specimens were cut into slices to determine a depth of penetration of sulfates from aggressive environments in concrete structure. The depth of penetration of the SO_3 - groups was measured using an electronic microscope equipped with microanalyzer REMMA 102-02.

Optimization of ratios of the main oxides of the binder, as well as of a composition of the binder-based coatings was performed using methods of numerical design of experiment. The calculations were performed using a program software product STATISTICA.

The conditions of work of the coatings in the sulfate environments were simulated by addition of the following sulfate salts, these: $MgSO_4$, Na_2SO_4, and $(NH_4)_2SO_4$ in the binder composition. Changes in pH-values of water extracts from the binders modified by the above salts during first four hours were measured using a laboratory apparatus "EZODO PL-700AL".

3. Results and discussions

3.1. Characterization of the hardened binders

3.1.1. The optimization of oxide ratios of the binder composition

The influence of oxide ratios of the binder composition on structure formation processes at normal temperatures was studied. In order to determine optimal oxide ratios of the binder in terms of strength and water resistance, a two factor- three level design of experiment was used. Chosen as variables were: SiO_2/Al_2O_3 and $K_2O/(Na_2O + K_2O)$ molar ratios. The design of experiment was divided into two parts, each part dealing with one of two binder compositions: $(Na_2O + K_2O)$•Al_2O_3•(2–4)•SiO_2·nH_2O and $(Na_2O + K_2O)$•Al_2O_3•(5–7)•SiO_2·nH_2O.

In order to obtain the zeolite-like reaction products with the enhanced resistance in sulfate environments the following proportions of the constituent oxides, these are: $(Na_2O + K_2O)/Al_2O_3 = 1$ and $SiO_2/Al_2O_3 = 2–7$ [73], have been chosen. Potassium oxide (K_2O) taken in quantities starting from 0 up to 0.3 mol, (correspondingly, the contents of Na_2O = 0.7–1.0 mol) was added in order to create the required conditions for a synthesis of the sodium–potassium zeolite-like phases [75].

In order to provide a similar viscosity of 18 cm measured by a viscometer acc. to Suttard, the values of H_2O/Al_2O_3 ratios were taken as constant.

Dependences of properties of the hardened binder from the ratios of constituent oxides were plotted (Fig. 1).

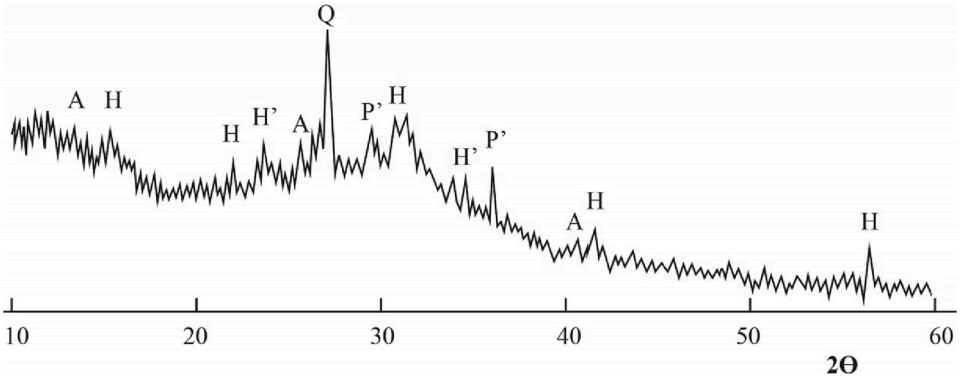

Fig. 2. XRD patterns of the hardened binder of the composition $(0.2K_2O + 0.8Na_2O)\cdot 4.5SiO_2\cdot Al_2O_3\cdot nH_2O$ after hardening for 90 days at t = 20 ± 2 °C and RH = 95 ± 5 %. Abbreviations: Q – quartz, C, C' – calcium silicate hydrates: $Ca_6Si_6O_{16}\cdot H_2O$ and $Ca_6Si_3O_{12}\cdot 2H_2O$, A – analcime, Sc – sodium-calcium silicate hydrate, Z – zeolite K-M, T – thompsonite, G – gismondine, H – heulandite-Na, H' – heulandite-K.

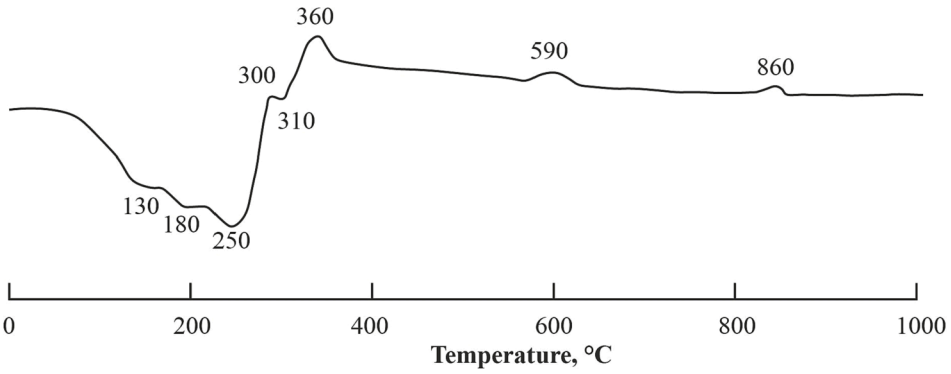

Fig. 3. DTA curves of the hardened binder of the composition $(0.2K_2O + 0.8Na_2O)\cdot 4.5SiO_2\cdot Al_2O_3\cdot nH_2O$ after hardening for 90 days at t = 20 ± 2 °C and RH = 95 ± 5 %.

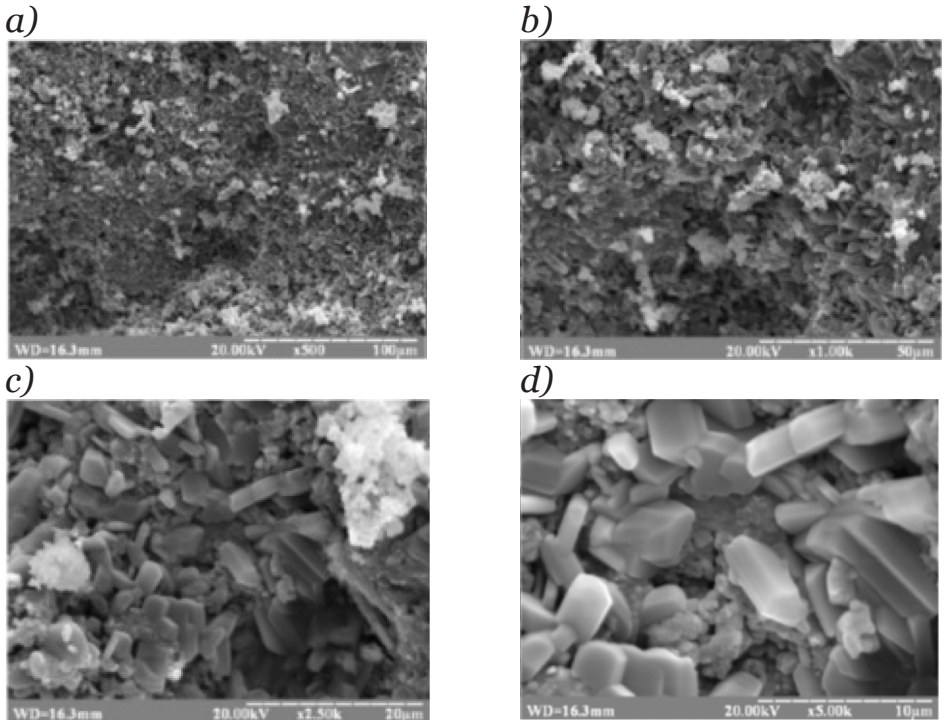

Fig. 4. Images of a cleavage surface (a) (electron microscopy) of the hardened binder of the composition $(0.2K_2O + 0.8Na_2O)\cdot 4.5SiO_2\cdot Al_2O_3\cdot nH_2O$ after hardening for 90 days at t = 20 ± 2 °C and RH = 95 ± 5 %. Magnification: a – ×500; b – ×1000; c – ×2500; d – ×5000.

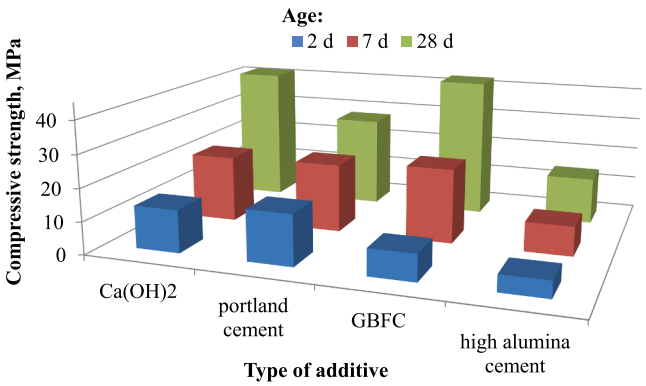

Fig. 5. Strength values of the hardened binder modified by calcium-containing additives vs. age at t = 20 ± 2 °C and RH = 95 ± 5 %.

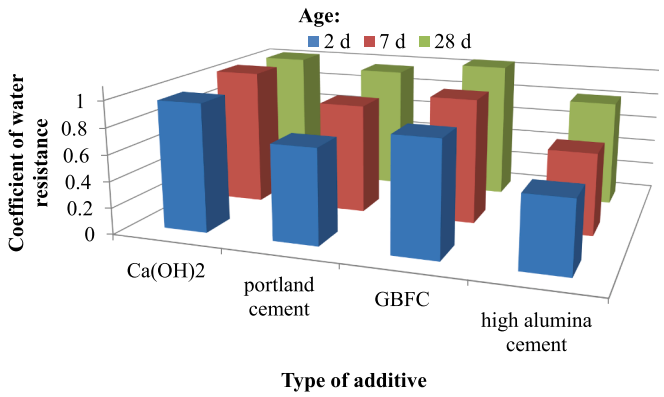

Fig. 6. Water resistance of the hardened binder vs. calcium-containing additives and age at t = 20 ± 2 °C and RH = 95 ± 5 %.

The highest values of compressive strength of 22–25 MPa after 28 days of hardening at normal temperatures can be achieved with the following ratios of constituent oxides in the binder: SiO_2/Al_2O_3 = 3.5–5.5 (Fig. 1a) and $K_2O/(Na_2O + K_2O)$ = 0.15–0.25 (Fig. 1b). The highest values of water resistance of the hardened binder ($K_w > 0.8$) can be achieved with the following ratios: SiO_2/Al_2O_3 = 4.5–5.5 and $K_2O/(Na_2O + K_2O)$ = 0.10–0.30.

The following ratios of constituent oxides, namely: SiO_2/Al_2O_3 = 4.5–5.0 and $K_2O/(Na_2O + K_2O)$ = 0.15–0.25, are found to be the best ratios of oxides in terms of strength and water resistance of the hardened binder.

Analysis of the reaction products of the binder of the composition $(0.2K_2O + 0.8Na_2O)\cdot 4.5SiO_2\cdot Al_2O_3\cdot nH_2O$ showed that, after hardening under normal conditions, the formation of zeolite-like minerals like analcime, heulandite-Na ($Na_6Si_{27}Al_{36}O_{72}\cdot 24H_2O$), heulandite-K ($(K_6Si_{27}Al_{36}O_{72}\cdot 24H_2O$) as well as phillipsite-(Na,K) ($(Na, K)_6(Al_6Si_{10}O_{32})\cdot 12H_2O$) can be assumed in the structure of the hardened binder (Fig. 2) [76].

The results of DTA complete the deduction of XRD. The DTA curve recorded a stepped dehydration of the hardened binder until 250 °C, what is typical for the zeolite-like minerals of the heulandite [77] and phillipsite [78] types, which is confirmed also by an *endo*-effect at 310 °C. Exo-effects (+) at temperatures 360, 590, and 860 °C indicate the presence of the zeolite-like minerals of the analcime type (Fig. 3) [79].

The images of microstructure demonstrate a dense structure of the hardened binder with sub-crystalline phases and a large number of crystalline phases. Heulandite phases are characterized by prismatic and plate crystals [77] and phillipsite phases are crystal-like ones (Fig. 4) [78].

3.1.2. The influence of calcium-containing additives properties of the hardened binder.

As was established, the use of the optimal composition of the binder, namely: $(0.2K_2O + 0.8Na_2O)\bullet 4.5SiO_2\bullet Al_2O_3\cdot nH_2O$, allows for to obtain a water resistant hardened alkali-activated material at 20 ± 2 °C. However, at the early ages of hardening, relatively low values of strength and water resistance can be achieved. In order to find a solution, the influence of the calcium-containing modifying additives as intensifiers of structure formation processes was studied.

Slaked lime, Portland cement, granulated blast furnace slag, high alumina cement were chosen as such modifying additives. These additives were added in quantities of 5 % of the binder by mass.

As it follows from Fig. 5, at early ages of hardening, the binder is characteristic of the highest strength in case of addition of slaked lime and Portland cement. However, at an age of 28 days the strength gained in case of slaked lime is by 49.0 % higher than that of the composition with Portland cement (27.9 MPa).

In case of the addition of granulated blast furnace slag a strength of the hardened binder at an age of 2 days is lower than those of the compositions with slaked lime by 37 % and Portland cement by 47 %. However, at an age of 7 days, the strength is by appr.10 % higher compared to those of the compositions with slaked lime and Portland cement. At an age of 28 days, the strength with the addition of GBFS is by 53 % higher than that of the composition with Portland cement, and almost similar to that of the composition with slaked lime.

The hardened binder of the composition with high alumina cement is characteristic of the lowest strength values; for example, at an age of 2 days the strength values are by 2.5–3.0 times lower than those of the compositions with slaked lime or Portland cement. This tendency can be observed during all ages of hardening under study.

Thus, in terms of strength characteristics of the hardened binder, the slaked lime is the best additive: it accelerates strength development at early ages and provides high strength values at an age of 28 days.

The use of calcium-containing modifying additives can provide a water resistance of the hardened binder at an age of 28 days after hardening at normal temperatures (Fig. 6). At the same time, a water resistance at the early ages can be achieved only with the additives of Portland cement, granulated blast furnace slag or slaked lime. The highest values of water resistance of the hardened alkali activated material ($K_w > 0.95$), in particular, at early ages and at an age of 28 days can be achieved by the use of the additive of slaked lime. The use of high alumina cement is not able to provide a required water resistance of the hardened binder even at an age of 7 days at normal temperatures.

This peculiarity can be attributed to a different phase composition of the reaction products represented by silicates, aluminates, aluminosilicates, and hydroxides. According to [80], a hydraulic activity of calcium silicates and aluminates depends upon crystallo - chemical specific features of structure and decreases, respectively, as follows: $3CaO\bullet SiO_2$ > β-$2CaO\bullet SiO_2$ > γ-$2CaO\bullet SiO_2$ > $3CaO\bullet 2SiO_2$ > $CaO\bullet 2SiO_2$ and $3CaO\bullet Al_2O_3$ > $12CaO\bullet 7Al_2O_3$ > $CaO\bullet Al_2O_3$ > $CaO\bullet 2Al_2O_3$. At early stages of hardening, the binder without modifying additives is represented by the N-A-S-H and K-A-S-H gels, as well as active anion groups in a form of the following tetrahedra, these are: $[AlO_4]^{5-}$ and $[SiO_4]^{4-}$. These tetrahedra, in the presence of an alkali metal compound solution, create the more complicated systems and in the process of condensation provides their valency compensation with the transformation into a state with a minimal reserve of free energy [61]. The zeolite-like alkaline aluminosilicate hydrates of sodium and potassium of the $N(K)AS_xH_y$ type are identified as reaction products.

A quick strength gain of the binder in case of the addition of Portland cement can be conjectured to a large content (>50 %) of tricalcium silicate $3CaO\bullet SiO_2$ (alite). It can be suggested that the interaction of alite with the alkaline components of the binder results in the early formation of the C-S-H gel with the higher degree of crystallinity. Under interaction of the C-S-H and N(K)-A-S-H gels and in the presence of the

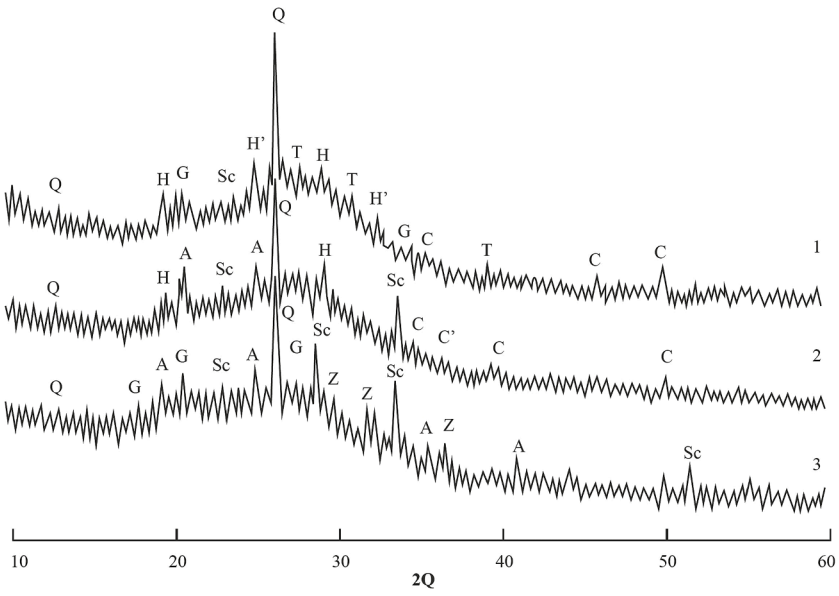

Fig. 7. The XRD patterns of the hardened binder of the following composition: $0.8Na_2O + 0.2K_2O)\cdot Al_2O_3\cdot 4.5SiO_2\cdot 15H_2O$ modified by the following additives: 1 – slaked lime, 2 – granulated blast furnace slag, 3 – Portland cement after hardening for 28 days t = 20 ± 2 °C and RH = 95 ± 5 %. Abbreviations: Q – quartz, C, C' – calcium silicate hydrates: $Ca_6Si_6O_{16}\cdot H_2O$ and $Ca_6Si_3O_{12}\cdot 2H_2O$, A – analcime, Sc – sodium-calcium silicate hydrate, Z – zeolite K-M, T – thompsonite, G – gismondine, H – heulandite-Na, H' – heulandite-K.

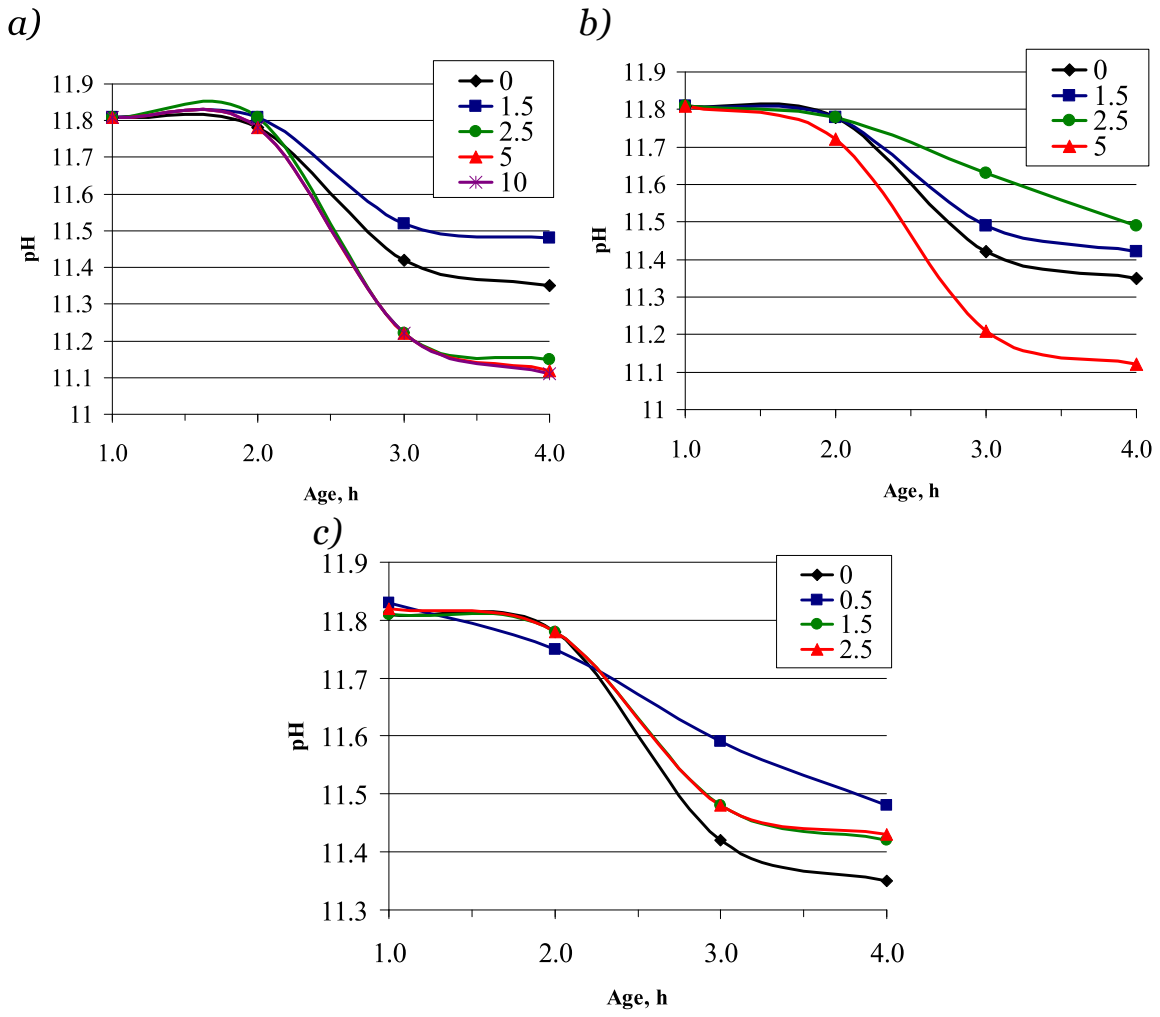

Fig. 8. The influence of contents of the following additives: $MgSO_4$ (a), $(NH_4)_2SO_4$ (b), and Na_2SO_4 (c) on changes in a pH-value of water extracts from the binder vs.age.

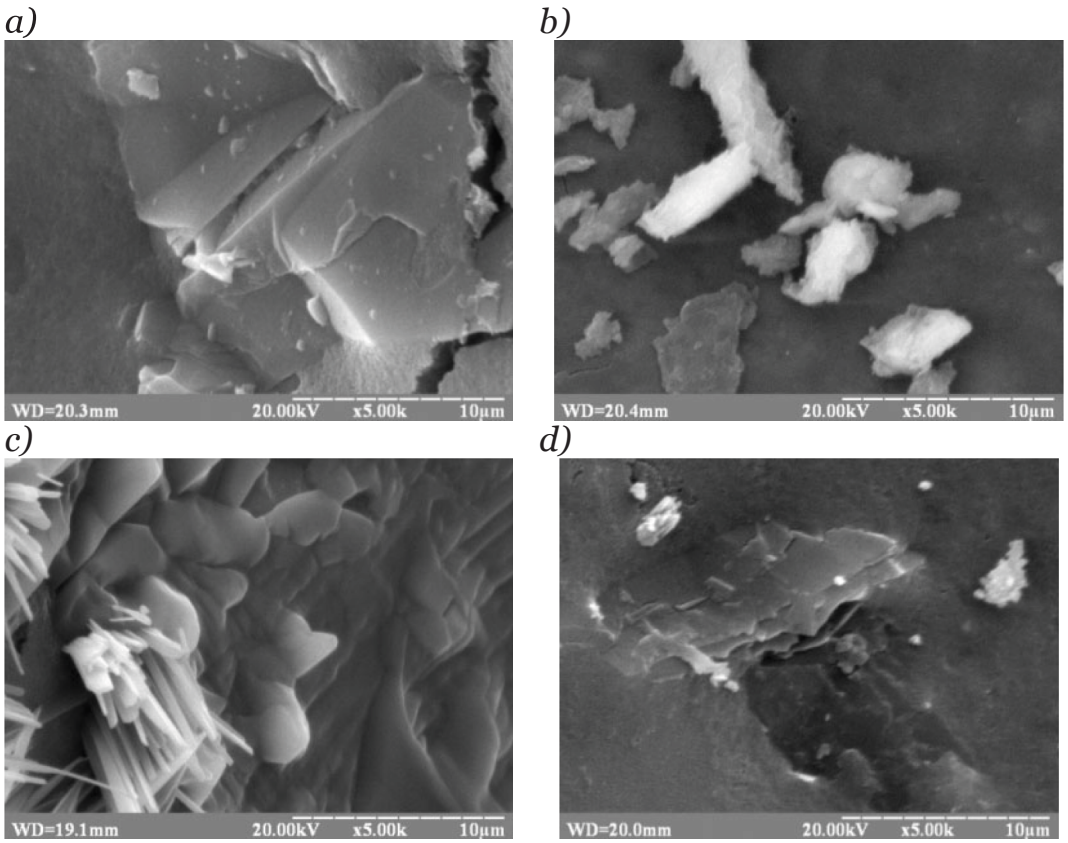

Fig. 9. SEM images of a cleavage surface of the binder without modifying additive (reference specimens)(a) and with the following modifying additives: sulfate of magnesium (b), ammonium (c) and sodium (d) added in a quantity of 2.5 % by mass after hardening for 180 days t = 20 ± 2 °C and RH = 95 ± 5 %.

following active groups, these are: $[AlO_4]^{5-}$ and $[SiO_4]^{4-}$, hybrid reaction products of the C-N-A-S-H and C-K-A-S-H types are formed [72]; this results in quick setting of the binder, leading, in its turn, to extremely quick strength gain and the occurrence of inhomogeneous structure of the hardened binder with low strength values.

The $CaO•Al_2O_3$ and $12CaO•7Al_2O_3$ are main aluminate phases of high alumina cement, which, according to [81], in the process of interaction with the alkali metal compounds and in the presence of amorphous silica, presumably produces aluminate hydrates of the CAH_x type and hydrogarnets C_3SAH_4. An assumption can be made that, in the process of interaction with the N(K)-A-S-H gel and $[AlO_4]^{5-}$ and $[SiO_4]^{4-}$ groups, the formation of the C-N(K)-A-S-H phases at normal temperatures is not possible. This can explain the formation of a not water resistant hardened binder with low strength characteristics.

The C-S-H gel and other low-basic calcium silicate hydrates are formed in the process of interaction of such main phases of the GBFS as $2CaO•SiO_2$, β-$2CaO•SiO_2$, and $3CaO•2SiO_2$ with the alkaline compounds in the presence of amorphous silica [82]. A basicity of silicate hydrates in this case is lower compared to that of the hydration products of Portland cement, thus being evidence of a possibility of the formation of hybrid sodium-calcium silicate hydrates [83]. This assumption is supported by the conclusions reported in [61]. With the silicate basicity lowering and in the presence of such active groups as $[AlO_4]^{5-}$ and $[SiO_4]^{4-}$ in the alkaline environment, the quantities of the resulted hydrid phases of the C-N(K)-A-S-H type tend to increase. High strength and water resistance can be attributed to the presence of these phases in the composition of the hardened binder [84].

3.1.3. The influence of calcium-containing additives on structure formation processes in the binder

Properties of the binder of optimal composition modified by calcium-containing additives are predetermined by a phase composition of the reaction products. The results of X-ray phase diffraction analysis of the specimens of the binder, modified by Ca-containing additives, which provide the highest water resistance and strength (i.e. slaked lime, Portland cement, granulated blast furnace slag), at an age of 28 days are given in Fig. 7.

It is conceivable a content of calcium silicate hydrates in the phase composition of the binder with slaked lime tends to decrease and contents of the zeolite-like phases of the gismondine ($CaSi_2Al_2O_8·4H_2O$), thompsonite ($NaCa_2(Al_5Si_5O_{20})·6H_2O$), heulandite-Na and heulandite-K types – to increase. The formation of the two latter mentioned hydrates creates preconditions for obtaining a corrosion resistant hardened alkali-activated material [73].

A phase composition of the hydrates in case of the addition of Portland cement supposedly is: zeolite-like minerals of the analcime, gismondine, zeolite K-M ($K_2Si_3Al_2O_{10}·3H_2O$) types [75], as well as sodium-calcium silicate hydrate ($Na_4Ca_4Si_6O_{18}·nH_2O$) and quartz (SiO_2).

The results of modification of the binder using granulated blast furnace slag can be described by the following phase composition: calcium silicate hydrates ($Ca_6Si_3O_{12}·2H_2O$ and $Ca_6Si_6O_{16}·H_2O$), sodium-calcium silicate hydrate and quartz, as well as the zeolite-like phases of the heulandite type [73].

3.2. Simulating a binding of the sulfate ions within a cement matrix

The incorporation of the sulfate ions in the mentioned zeolite-like reaction products of the binder can be assumed by the regularities under which the pH-values of water extracts change (Fig. 8) [85].

The slaked lime (2.0 % by mass) was used as a calcium-containing modifying additive of the binder of the following oxide composition $(0.2K_2O + 0.8Na_2O)•4.5SiO_2•Al_2O_3·nH_2O$ [86]. In order to simulate an intensity of binding of the sulfate ions depending upon a cation of sulfate

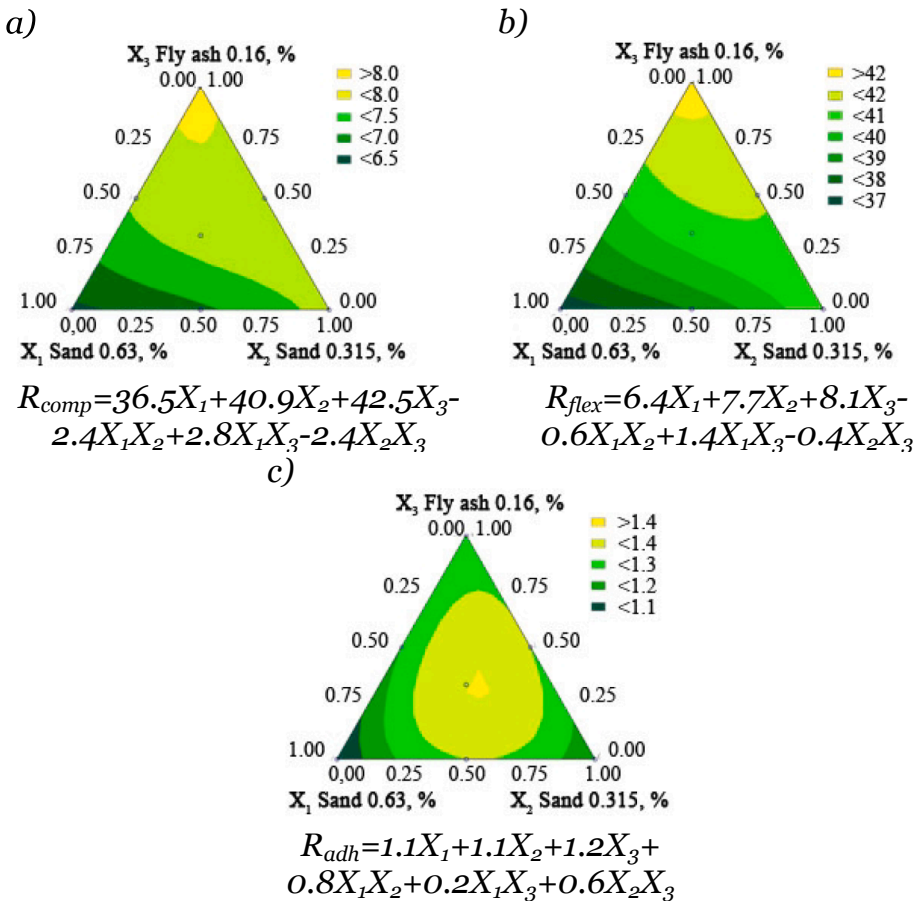

Fig. 10. Projections of response surfaces of strength changes of the coatings: flexural (a), compressive (b) and adhesion to a concrete substrate (c) vs. the fractional composition of the filler.

salts $MgSO_4$, $(NH_4)_2SO_4$, and Na_2SO_4 were used.

The addition of $MgSO_4$ in a quantity of appr. 2.5 % results in the lower pH-values compared to those of the reference composition (without additive) (Fig. 8a). This is evidence of a more intensive flow of chemical reaction in the binder and possibility of crystallization of the zeolite-like aluminosilicate hydrates at normal temperatures. The magnesium ions participate, side by side with the calcium (Ca^{2+}) - ions, in their formation and bind the sulfate ions. This trend (reduction of pH-values in case of the addition of $(NH_4)_2SO_4$ is almost observed even at content at a level of 5 %, this being evidence of the flow of structure formation processes in the same direction. However, as soon as the speed of these processes decelerates due to the lowering concentration of the alkali earth metals in the system, other types of zeolite-like structures can be formed (Fig. 8b). The addition of Na_2SO_4 almost does not change the intensity of structure formation processes due to the absence of cation exchange. Stability of the pH-values within a dosage range (0.5–2.5 %) under study supports this conclusion (Fig. 8c).

A resistance of the coatings based on the proposed aluminosilicate binders in sulfate environments can be attributed to the formation of the zeolite-like reaction products, which contain such ions as sulfate anions and sodium cations. It can be assumed the exchange of the hydroxyl ions and sulfate ions result in the formation of following zeolite-like minerals: without calcium – nosean ($Na_8(Al_6Si_6O_{24})(SO_4)\cdot H_2O$), pitiglianoite ($Na_6K_2(Al_6Si_6O_{24})(SO_4)\cdot 2H_2O$), vishnevite ((Na,K)$_8(Al_6Si_6O_{24})(SO_4,CO_3)\cdot 2H_2O$) as well as containing one – cancrinite ((Na,Ca)$_8(Al_6Si_6)O_{24}(CO_3,SO_4)_2\cdot$2H2O), biachellaite ((Na,Ca,K)$_8(Si_6Al_6O_{24})(SO_4)_2$ $(OH)_{0.5}\cdot H_2O$), franzinite ((Na,K)$_6Ca_2(Al_6Si_6O_{24})(SO_4)_2\cdot 0.5H_2O$), farneseite ((Na,K, Ca)$_{56}(Al_6Si_6O_{24})_7(SO_4)_{12}\cdot 6H_2O$). In its turn, the exchange of sodium cation and ammonium or magnesium cations could conceivably lead to a synthesis of such phases as, for example, heilandite-NH_4 ($[(NH_4)_2Ca]_2Al_4Si_{14}O_3\cdot 12H_2O$), chabasite-$NH_4$ ($[(NH_4)_2Ca]Al_2Si_4O_{12}\cdot 6H_2O$), thompsonite-$NH_4$ ((Na,NH_4)$Ca_2[Al_5Si_5O_{20}]\cdot 6H_2O$), faujasite-Mg ((Mg,$Na_2$, Ca)$_{3.5}[Al_7Si_{17}O_{48}]\cdot 32H_2O$), chabasite-Mg ($(Mg_{0.7}K_{0.5}Ca_{0.5}Na_{0.1})[Al_3Si_9O_{24}]\cdot$ $\cdot 10H_2O$), ferrierite-Mg ((Mg,Na_2,K_2,Ca)$_{3\text{-}5}$Mg$[Al_{5\text{-}7}Si_{27.5\text{-}31}O_{72}]\cdot 18H_2O$) [76,87].

The «restrictions» placed on transport of the sulfate ions can be caused not only by their incorporating in the zeolite-like hydrates but also by an additional increase of a degree of crystallization in the presence of ammonium and magnesium cations as well; this statement is supported by the data of the electron microscopy (Fig. 9).

3.3. Optimization of a mixture design of the protective coating

A proper choice of the appropriate fillers is a key factor with regard to the structure formation of the coatings based on the binder and determines technology-related parameters of the resulted mortar [88].

In order to make optimization of the composition of the coatings in terms of flexural and compressive strength values, as well as adhesion strength to a concrete substrate after 28 days of hardening a ternary mixture design of experiment was planned and used. The consistency values measured as a flow of the mortar was 20 ± 2 cm. The chosen variables (factors) were: factor X_1 – the content of sand fr. 0.315–0.63 mm (real values – 35–50 % by mass), factor X_2 – the content of sand fr.0–0.315 mm (30–45 % by mass) and factor X_3 – the content of fly ash fr. ≤ 0.16 mm (20–35 % by mass).

The contents of other ingredients in the composition of the coating are, in % of the binder by mass: slaked lime – 2.5, carboxymethylcellulose – 0.16, trisodiumphosphate – 2.5, sodium gluconate – 1, basalt mica – 1.6.

Projections of response surfaces of properties of the coatings,

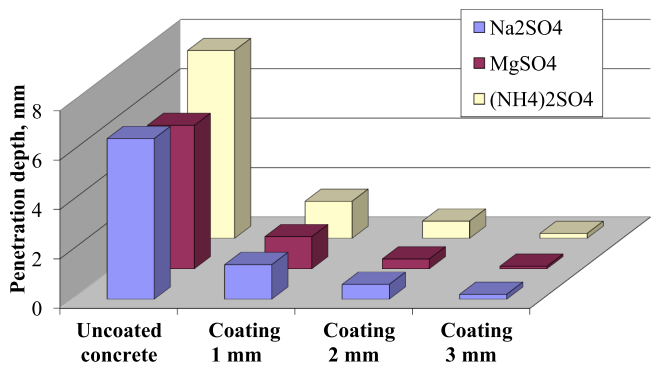

Fig. 11. Depth of penetration of sulfate ions into the uncoated and coated (1, 2, 3 mm) concrete after 360 days in aggressive environments.

depending upon the fractional content of the filler, were plotted (Fig. 10).

The formulated optimal mixture design of the coating based on the binder is characteristic of the norm-specified technology-related and performance properties: consistency (flow) –≥20 cm, consistency retention –≥90 min., water-retaining ability –≥95%, compressive strength –≥40.0 MPa, flexural strength –≥8.0 MPa, the strength of adhesion to a concrete substrate –≥1.2 MPa, grade in water impermeability – W10, grade in freeze/thaw resistance – F300.

3.4. Protective properties of the coating

Protective properties of the coating of the optimal mixture design can be evaluated by a depth of penetration of the sulfate ions from aggressive environments into a concrete substrate. The uncoated concrete substrate, depending upon a cation of the sulfate salt, is characteristic of a depth of penetration of the sulfate ions of 5.8–7.6 mm; on the contrary, the coated concrete substrate– 0.1–1.5 mm, depending upon a thickness of the coating (Fig. 11).

As it follows, when the coating is applied in a thickness of 1 mm, the depth of penetration of the sulfate ions of the sodium sulfate into a concrete substrate is 1.3–1.5 mm. The larger thickness of the coating (up to 3 mm) makes the transport of the sulfate ions into a concrete substrate almost impossible; this conclusion is supported by the results of the electron microprobe analysis. As follows from Fig. 12a, the depth of penetration of the sulfates into the uncoated concrete substrate is 2.4 mm. In the case of the coated (3 mm) concrete substrate, no sulfates were found (Fig. 12b).

According to the study results, the following regularity can be observed in terms of reduction of the depth of penetration of the sulfate ions into the coated concrete substrate: $(NH_4)_2SO_4 > Na_2SO_4 > MgSO_4$; this can be attributed to a chemical activity of cations of the salts.

4. Conclusions

1. The results of the study showed a possibility to prevent corrosion of reinforced concrete constructions under attacks of the following sulfate environments, these are: $MgSO_4$, $(NH_4)_2SO_4$ and Na_2SO_4, by using the coatings based on the alkaline aluminosilicate binder of the Na_2O-K_2O-Al_2O_3-SiO_2-H_2O system. These coatings are intended to be applied on the concrete surface and they are capable to bind sulfate ions and eliminate both the possibility of attacks of the sulfate environments on a concrete structure and the risk of corrosion of steel reinforcement.

2. The conditions for the synthesis of water-resistant zeolite-like matrices of the analcime ($NaAlSi_2O_6{\cdot}H_2O$), heulandite-Na ($Na_6Si_{27}Al_{36}O_{72}{\cdot}24H_2O$), heulandite-K ($K_6Si_{27}Al_{36}O_{72}{\cdot}24H_2O$), phillipsite-(Na,K) ($(Na,K)_6(Al_6Si_{10}O_{32}){\cdot}12H_2O$) and zeolite K-M ($K_2Si_3Al_2O_{10}{\cdot}3H_2O$) types are formed at 20 ± 2 °C at SiO_2/Al_2O_3 = 4–5 and $K_2O/(Na_2O + K_2O)$ = 0.15–0.30. These matrices have high sulfate resistance and are able to bind through chemical adsorption (in pores) or chemical reaction the sulfate ions in the zeolite-like phases. The higher degree of crystallization of these phases in the presence of sulfate cations can initiate the effect of self-healing.

3. The speed with which the sulfate ions are bound in the coating depends upon a chemical activity of a cation of the sulfate environment and increases as the following: $(NH_4)_2SO_4 < Na_2SO_4 < MgSO_4$.

4. The addition of calcium-containing modifying additives, such as Portland cement, slaked lime, granulated blast furnace slag, is found to accelerate the synthesis of water-resistant zeolite-like matrices at 20 ± 2 °C. This acceleration can be attributed to an additional formation of gismondine ($CaSi_2Al_2O_8{\cdot}4H_2O$), thompsonite ($NaCa_2(Al_5Si_5O_{20}){\cdot}6H_2O$) and other zeolite-like phases, depending upon a cation of the sulfate environment.

5. An optimal mixture of the coating was designed using a ternary mixture design of experiment. This optimal mixture design, when the coating is applied on a concrete surface in a thickness of 3 mm, prevents completely corrosion of concrete and transport of sulfate ions from solutions of sodium, magnesium and ammonium sulfates into the depth of concrete.

CRediT authorship contribution statement

Pavel Krivenko: Conceptualization, Funding acquisition, Project administration, Supervision, Validation, Writing – review & editing. **Igor Rudenko:** Data curation, Formal analysis, Investigation, Methodology, Resources, Software, Visualization, Writing – original draft. **Oleksandr Konstantynovskyi:** Data curation, Formal analysis, Investigation, Methodology, Resources, Software, Visualization, Writing – original draft. **Danutė Vaičiukynienė:** Conceptualization, Funding acquisition, Project administration, Supervision, Validation, Writing – review & editing.

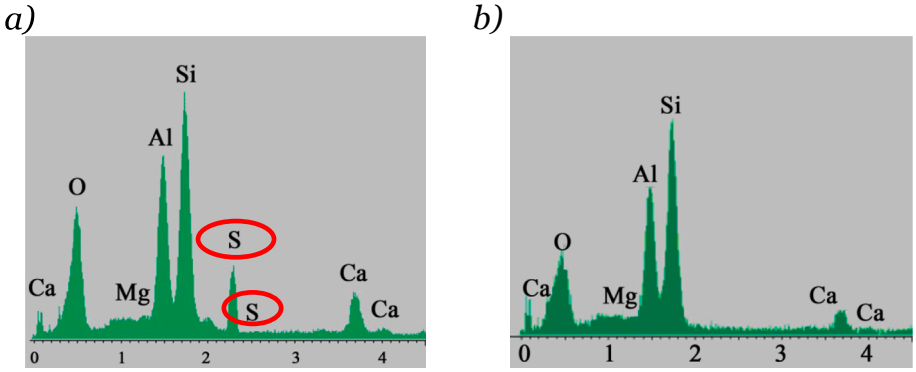

Fig. 12. Elemental distribution of the uncoated (a) and the coated (3.0 mm) (b) concrete substrate after storage for 360 days in a sodium sulfate solution.

Declaration of Competing Interest

The authors declare the following financial interests/personal relationships which may be considered as potential competing interests:

Konstantynovskyi Oleksandr reports administrative support was provided by Kyiv National University of Construction and Architecture.

The remaining authors declare that they have no known competing financial interests or personal relationships that could have appeared to influence the work reported in this paper.

Data availability

The data that has been used is confidential.

Acknowledgments

Authors would like to acknowledge the contribution of the Research Council of Lithuania and the Ministry of Education and Science of Ukraine project "Solutions to reduce aggressive ions SO_4^{2-} and Cl^- during transport in Portland cement concrete with steel reinforcement in hydraulic structures", project code S-LU-22-7. The authors also express their gratitude to the Ministry of Education and Science of Ukraine for financial support of this research that is carried out within the budgetary financing of topic with registration No 1020U001010 and implementation period of 2020-2022.

References

[1] M. Alexander, H. Beushausen, Durability, service life prediction, and modelling for reinforced concrete structures – review and critique, Cem. Concr. Res. 122 (2019) 17–29, https://doi.org/10.1016/j.cemconres.2019.04.018.
[2] J.Y. Hu, S.S. Zhang, E. Chen, W.G. Li, A review on corrosion detection and protection of existing reinforced concrete (RC) structures, Constr. Build. Mater. 325 (2022), 126718, https://doi.org/10.1016/j.conbuildmat.2022.126718.
[3] H. Zhao, Y. Hu, Z. Tang, K. Wang, Y. Li, W. Li, Deterioration of concrete under coupled aggressive actions associated with load, temperature and chemical attacks: a comprehensive review, Constr. Build. Mater. 322 (2022), 126466, https://doi.org/10.1016/j.conbuildmat.2022.126466. Elsevier Ltd.
[4] Y. Kitsutaka, M. Tsukagoshi, Method on the aging evaluation in nuclear power plant concrete structures, Nucl. Eng. Des. 269 (2014) 286–290, https://doi.org/10.1016/j.nucengdes.2013.08.041.
[5] Y. Yi, D. Zhu, S. Guo, Z. Zhang, C. Shi, A review on the deterioration and approaches to enhance the durability of concrete in the marine environment, Cem. Concr. Compos. 113 (2020), 103695, https://doi.org/10.1016/j.cemconcomp.2020.103695.
[6] Q. Liu, M. Huang, F. Jin, Study on durability and service life of concrete structure of coastal tunnel, Beijing Jiaotong Daxue Xuebao, J. Beijing Jiaotong Univ. 42 (6) (2018) 1–8. https://doi.org/10.11860/j.issn.1673-0291.2018.06.001.
[7] J. Sulikowski, J. Kozubal, The durability of a concrete sewer pipeline under deterioration by sulphate and chloride corrosion, Procedia Eng. 153 (2016) 698–705, https://doi.org/10.1016/j.proeng.2016.08.229.
[8] E. Menéndez, T. Matschei, F.P. Glasser, Sulfate attack of concrete, in: M. Alexander., A. Bertron, N. De Belie (Eds), Performance of cement-based materials in aggressive aqueous environments, RILEM State-of-the-Art Reports, 10 (2013) 7–74. https://doi.org/10.1007/978-94-007-5413-3_2.
[9] P. Xu, L. Jiang, M.Z. Guo, J. Zha, L. Chen, C. Chen, N. Xu, Influence of sulfate salt type on passive film of steel in simulated concrete pore solution, Constr. Build. Mater. 223 (2019) 352–359, https://doi.org/10.1016/j.conbuildmat.2019.06.209.
[10] T. Aye, C.T. Oguchi, Resistance of plain and blended cement mortars exposed to severe sulfate attacks, Constr. Build. Mater. 25 (6) (2011) 2988–2996, https://doi.org/10.1016/j.conbuildmat.2010.11.106.
[11] J. Stark, B. Wicht, Dauerhaftigkeit von Beton: der Baustoff als Werkstoff, Birkhäuser, Berlin, 2001.
[12] M. Maes, N. De Belie, Resistance of concrete and mortar against combined attack of chloride and sodium sulphate, Cem. Concr. Compos. 53 (2014) 59–72, https://doi.org/10.1016/j.cemconcomp.2014.06.013.
[13] A. Goyal, H.S. Pouya, E. Ganjian, P. Claisse, A review of corrosion and protection of steel in concrete, Arab. J. Sci. Eng. 43 (2018) 5035–5055, https://doi.org/10.1007/s13369-018-3303-2.
[14] L. Bertolini, B. Elsener, P. Pedeferri, E. Redaelli, R.B. Polder, Corrosion of Steel in Concrete: Prevention, Diagnosis, Repair, John Wiley & Sons, Oxford, 2013.
[15] X. Pan, Z. Shi, C. Shi, T.-C. Ling, N. Li, A review on surface treatment for concrete – Part 2: performance, Constr. Build. Mater. 133 (2017) 81–90, https://doi.org/10.1016/j.conbuildmat.2016.11.128.
[16] G. De Schutter, in: Damage to Concrete Structures, 1st ed., CRC Press, London, 2012 https://doi.org/10.1201/b12914.
[17] C. Xiong, L. Jiang, Y. Xu, H. Chu, M. Jin, Y. Zhang, Deterioration of pastes exposed to leaching, external sulfate attack and the dual actions, Constr. Build. Mater. 116 (2016) 52–62, https://doi.org/10.1016/j.conbuildmat.2016.04.133.
[18] J. Wu, W. Zhu, J. Wei, M. Tang, S. Zhang, X. Zhang, A comparable study on the deterioration of concrete under sodium sulfate and magnesium sulfate attack, IOP Conf. Ser.: Earth Environ. Sci. 787 (2021), 012037. 10.1088/1755-1315/787/1/012037.
[19] S. Babu, K.P. Ramaswamy, M. Nazeer, A review on the deterioration of cement-based materials in ammonium salt solutions, IOP Conf. Ser.: Earth Environ. Sci. 491 (1) (2020), 012041, https://doi.org/10.1088/1755-1315/491/1/012041.
[20] J. Wang, D. Niu, Y. Wang, B. Wang, Durability performance of brine-exposed shotcrete in salt lake environment, Constr. Build. Mater. 188 (2018) 520–536, https://doi.org/10.1016/j.conbuildmat.2018.08.139.
[21] M. Harilal, R.P. George, J. Philip, S.K. Albert, Binary blended fly ash concrete with improved chemical resistance in natural and industrial environments, Environ. Sci. Pollut. Res. 28 (2021) 28107–28132, https://doi.org/10.1007/s11356-021-12453-4.
[22] M.A. Elahi, C.R. Shearer, A.N.R. Reza, A.K. Saha, M.N.N. Khan, M.A. Hossain, P. K. Sarker, Improving the sulfate attack resistance of concrete by using supplementary cementitious materials (SCMs): a review, Constr. Build. Mater. 281 (2021), 122628, https://doi.org/10.1016/j.conbuildmat.2021.122628.
[23] P. Krivenko, I. Rudenko, O. Konstantynovskyi, Design of slag cement, activated by Na (K) salts of strong acids, for concrete reinforced with steel fittings, Eastern-Eur. J. Enterprise Technol. 6 (6–108) (2020) 26–40. https://doi.org/10.15587/1729-4061.2020.217002.
[24] M. Sanytsky, A. Usherov-Marshak, T. Kropyvnytska, I. Heviuk, Performance of multicomponent portland cements containing granulated blast furnace slag, zeolite, and limestone, Cem. Wapno Beton 2020 (5) (2020) 416–427. https://doi.org/10.32047/CWB.2020.25.5.7.
[25] M. Sanytsky, T. Kropyvnytska, S. Fic, H. Ivashchyshyn, Sustainable low-carbon binders and concretes, E3S Web Conf. 166 (2020) 06007, https://doi.org/10.1051/e3sconf/202016606007.
[26] P. Krivenko, I. Rudenko, O. Konstantynovskyi, D. Vaičiukynienė, Mitigation of corrosion initiated by Cl^- and SO_4^{2-}-ions in blast furnace cement concrete mixed with sea water, Materials 15 (9) (2022) 3003, https://doi.org/10.3390/ma15093003.
[27] K. Devi, P. Aggarwal, B. Saini, Admixtures used in self-compacting concrete: a review, Iran. J. Sci. Technol. Trans. Civ. Eng. 44 (2020) 377–403, https://doi.org/10.1007/s40996-019-00244-4.
[28] R. Raj, M. Bhat, A. Agrawal, N. Chandak, Review on the durability parameters of self-compacting concrete, Adv. Constr. Mater. Sustain. Environ. Lecture Notes Civ. Eng. 196 (2022) 219–238, https://doi.org/10.1007/978-981-16-6557-8_18.
[29] O.P. Nikiforov, High-density concrete based on slag-containing binders with complex modifiers: Monograph, Porogi, Dnipropetrovsk, 1996.
[30] M. Palacios, Y.F. Houst, P. Bowen, F. Puertas, Adsorption of superplasticizer admixtures on alkali-activated slag pastes, Cem. Concr. Res. 39 (8) (2009) 670–677, https://doi.org/10.1016/j.cemconres.2009.05.005.
[31] P. Krivenko, I. Rudenko, O. Konstantynovskyi, Comparison of influence of surfactants on the thermokinetic characteristics of alkali-activated slag cement, Eastern-Eur. J. Enterprise Technol. 6 (6–114) (2021) 24–32. https://doi.org/10.15587/1729-4061.2021.245916.
[32] P. Krivenko, V. Gots, O. Petropavlovskyi, I. Rudenko, O. Konstantynovskyi, The influence of complex additive on strength and proper deformations of alkali-activated slag cements, Mater. Sci. Forum 968 (2019) 13–19, https://doi.org/10.4028/www.scientific.net/MSF.968.13.
[33] P. Krivenko, V. Gots, O. Petropavlovskyi, O. Konstantynovskyi, A. Kovalchuk, Development of solutions concerning regulation of proper deformations in alkali-activated cements, Eastern-Eur. J. Enterprise Technol. 5 (6–101) (2019) 24–32. https://doi.org/10.15587/1729-4061.2019.181150.
[34] P. Krivenko, V. Gots, O. Petropavlovskyi, I. Rudenko, O. Konstantynovskyi, Complex shrinkage-reducing additives for alkali activated slag cement fine concrete, Solid State Phenomena 321 SSP (2021) 165–170. https://doi.org/10.4028/www.scientific.net/SSP.321.165.
[35] P. Krivenko, O. Petropavlovskyi, O. Kovalchuk, I. Rudenko, O. Konstantynovskyi, Enhancement of alkali-activated slag cement concretes crack resistance for mitigation of steel reinforcement corrosion, E3S Web Conf. 166 (2020) 06001, https://doi.org/10.1051/e3sconf/202016606001.
[36] P. Krivenko, I. Rudenko, O. Petropavlovskyi, O. Konstantynovskyi, A. Kovalchuk, Alkali-activated portland cement with adjustable proper deformations for anchoring application, IOP Conf. Ser.: Mater. Sci. Eng. 708 (1) (2019), 012090, https://doi.org/10.1088/1757-899X/708/1/012090.
[37] P. Krivenko, O. Petropavlovskyi, I. Rudenko, O. Konstantynovskyi, A. Kovalchuk, Complex multifunctional additive for anchoring grout based on alkali-activated portland cement, IOP Conf. Ser.: Mater. Sci. Eng. (MSE) 907 (2020), 012055, https://doi.org/10.1088/1757-899X/907/1/012055.
[38] M.V. Diamanti, A. Brenna, F. Bolzoni, M. Berra, T. Pastore, M. Ormellese, Effect of polymer modified cementitious coatings on water and chloride permeability in concrete, Constr. Build. Mater. 49 (2013) 720–728, https://doi.org/10.1016/j.conbuildmat.2013.08.050.
[39] J. Dai, Y. Akira, F.H. Wittmann, H. Yokota, P. Zhang, Water repellent surface impregnation for extention of service life of reinforced concrete structures in marine environments: the role of cracks, Cem Concr. Comp. 32 (2010) 101–109, https://doi.org/10.1016/j.cemconcomp.2009.11.001.
[40] A.A. Plugin, O.S. Borziak, O.A. Pluhin, T.A. Kostuk, D.A. Plugin, Hydration products that provide water-repellency for Portland cement-based waterproofing

compositions and their identification by physical and chemical methods, Lecture Notes Civ. Eng. 100 (2021), https://doi.org/10.1007/978-3-030-57340-9_40.
[41] M. Medeiros, P. Helene, Efficacy of surface hydrophobic agents in reducing water and chloride ion penetration in concrete, Mater. Struct. 41 (1) (2008) 59–71, https://doi.org/10.1617/s11527-006-9218-5.
[42] R.S. Woo, H. Zhu, M.M. Chow, C.K. Leung, J. Kim, Barrier performance of silane-clay nanocomposite coatings on concrete structure, Compos. Sci. Technol. 68 (14) (2008) 2828–2836, https://doi.org/10.1016/j.compscitech.2007.10.028.
[43] C.K. Leung, H. Zhu, J. Kim, R.S. Woo, Use of polymer/organoclay nanocomposite surface treatment as water/ion barrier for concrete, J. Mater. Civ. Eng. 20 (7) (2008) 484–492, https://doi.org/10.1061/(ASCE)0899-1561(2008)20:7(484).
[44] M. Delucchi, A. Barbucci, G. Cerisola, Study of the physico-chemical properties of organic coatings for concrete degradation control, Constr. Build. Mater. 11 (7) (1997) 365–371, https://doi.org/10.1016/S0950-0618(97)00060-3.
[45] E. Franzoni, B. Pigino, C. Pistolesi, Ethyl silicate for surface protection of concrete: performance in comparison with other inorganic surface treatments, Cem. Concr. Compos. 44 (2013) 69–76, https://doi.org/10.1016/j.cemconcomp.2013.05.008.
[46] M.A.R. Bhutta, T. Maruya, K. Tsuruta, Use of polymer-impregnated concrete permanent form in marine environment: 10-year outdoor exposure in Saudi Arabi, Constr. Build. Mater. 43 (2013) 50–57, https://doi.org/10.1016/j.conbuildmat.2013.01.028.
[47] A.M. Aguirre-Guerrero, R.M. de Gutiérrez, Alkali-activated protective coatings for reinforced concrete exposed to chlorides, Constr. Build. Mater. 268 (2021), 121098, https://doi.org/10.1016/j.conbuildmat.2020.121098.
[48] M. Sánchez, P. Faria, L. Ferrara, E. Horszczaruk, H.M. Jonkers, A. Kwiecień, J. Mosa, A. Peled, A.S. Pereira, D. Snoeck, M. Stefanidou, T. Stryszewska, B. Zajac, External treatments for the preventive repair of existing constructions: a review, Constr. Build. Mater. 193 (2018) 435–452, https://doi.org/10.1016/j.conbuildmat.2018.10.173.
[49] X. Pan, Z. Shi, C. Shi, T.-C. Ling, N. Li, A review on concrete surface treatment Part I: types and mechanisms, Constr. Build. Mater. 132 (2017) 578–590, https://doi.org/10.1016/j.conbuildmat.2016.12.025.
[50] P. Balaguru, M. Nazier, M. Arafa, Field implementation of geopolymer coatings. Project report of Center for Advanced Infrastructure and Transportation (CAIT). Civil and Environmental Engineering Piscataway, NJ: Rutgers State University, 2008.
[51] L. Biondi, M. Perry, C. Vlachakis, Z. Wu, A. Hamilton, J. McAlorum, Ambient cured fly ash geopolymer coatings for concrete, Materials 12 (6) (2019) 923, https://doi.org/10.3390/ma12060923.
[52] S. Sikora, E. Gapys, B. Michalowski, T. Horbanowicz, M. Hynowski, Geopolymer coating as a protection of concrete against chemical attack and corrosion, E3S Web Conf. 49 (2018) 00101, https://doi.org/10.1051/e3sconf/20184900101.
[53] Y. Zarina, A.M.M. Al Bakri, H. Kamarudin, I.K. Nizar, A.R. Rafiza, Reviews on the geopolymer materials for coating application, Adv. Mat. Res. 626 (2013) 958–962, https://doi.org/10.4028/www.scientific.net/AMR.626.958.
[54] A.M. Aguirre-Guerrero, R.A. Robayo-Salazar, R.M. de Gutiérrez, A novel geopolymer application: coatings to protect reinforced concrete against corrosion, Appl. Clay Sci. 135 (2017) 437–446, https://doi.org/10.1016/j.clay.2016.10.029.
[55] Z. Zhang, X. Yao, H. Zhu, Potential application of geopolymers as protection coatings for marine concrete, I. Basic properties, Appl. Clay Sci. 49 (1–2) (2010) 1–6, https://doi.org/10.1016/j.clay.2016.10.029.
[56] Z. Zhang, X. Yao, H. Zhu, Potential application of geopolymers as protection coatings for marine concrete: II Microstructure and anticorrosion mechanism, Appl. Clay Sci. 49 (1–2) (2010) 7–12, https://doi.org/10.1016/j.clay.2010.04.024.
[57] Y.W. Mao, L. Biasetto, P. Colombo, Metakaolin-based geopolymer coatings on metals by airbrush spray deposition, J. Coat. Technol. Res. 17 (2020) 991–1002, https://doi.org/10.1007/s11998-019-00310-6.
[58] P.V. Krivenko, S.G. Guzii, O.P. Bondarenko, Alkaline aluminosilicate binder-based adhesives with increased fire resistance for structural timber elements, Key Eng. Mater. 808 (2019) 172–176, https://doi.org/10.4028/www.scientific.net/KEM.808.172.
[59] S. Guzii, P. Krivenko, O. Bondarenko, T. Kopylova, Study on physico-mechanical properties of the modified alkaline aluminosilicate adhesive-bonded timber elements, Solid State Phenom. 296 (2019) 112–117, https://doi.org/10.4028/www.scientific.net/SSP.296.112.
[60] D.S.R. Rego, K.C. Gomes, A.F. Leal, N.P. Barbosa, S.M. Torres, D.S. Barros, Adhesion of ceramic plates with geopolymer, Mater. Sci. Forum 643 (2010) 139–142, https://doi.org/10.4028/www.scientific.net/MSF.643.139.
[61] P.V. Krivenko, Why alkaline activation – 60 years of the theory and practice of alkali-activated materials, J. Ceram. Sci. Technol. 8 (2017) 323–334, https://doi.org/10.4416/JCST2017-00042.
[62] P. Rozek, M. Krol, W. Mozgawa, Geopolymer-zeolite composites: a review, J. Clean. Prod. 230 (2019) 557e579, https://doi.org/10.1016/j.jclepro.2019.05.152.
[63] B.I. El-Eswed. Aluminosilicate Inorganic Polymers (Geopolymers): Emerging Ion Exchangers for Removal of Metal Ions. In: Inamuddin, Ahamed, M., Asiri, A. (eds) Applications of Ion Exchange Materials in the Environment. Springer, Cham. (2019) 65–93. https://doi.org/10.1007/978-3-030-10430-6_4.
[64] A.A. Siyal, M.R. Shamsuddin, M.I. Khan, N.E. Rabat, M. Zulfiqar, Z. Man, J. Siame, K.A. Azizli, A review on geopolymers as emerging materials for the adsorption of heavy metals and dyes, J. Environ. Manag. 224 (2018) 327e339, https://doi.org/10.1016/j.jenvman.2018.07.046.
[65] X. Niu, Y. Elakneswaran, C.R. Islam, J.L. Provis, T. Sato, Adsorption behaviour of simulant radionuclide cations and anions in metakaolin-based geopolymer, J. Hazard. Mater. 429 (2022), 128373, https://doi.org/10.1016/j.jhazmat.2022.128373.
[66] M. Minelli, E. Papa, V. Medri, F. Miccio, P. Benito, F. Doghieri, E. Landi, Characterization of novel geopolymer e zeolite composites as solid adsorbents for CO_2 capture, Chem. Eng. J. 341 (2018) 505e515, https://doi.org/10.1016/j.cej.2018.02.050.
[67] A. Haan, H. Eral, B. Schuur, Chapter 6. Adsorption and Ion Exchange. Industrial Separation Processes: Fundamentals, De Gruyter, Berlin, Boston, 2020, pp. 155–194. https://doi.org/10.1515/9783110654806-006.
[68] C. Fu, H. Ye, K. Zhu, D. Fang, J. Zhou, Alkali cation effects on chloride binding of alkali-activated fly ash and metakaolin geopolymers, Cem. Concr. Compos. 114 (2020), 103721, https://doi.org/10.1016/j.cemconcomp.2020.103721.
[69] P. He, Q. Wang, S. Fu, M. Wang, S. Zhao, X. Liu, Y. Jiang, D. Jia, Y. Zhou, Hydrothermal transformation of geopolymers to bulk zeolite structures for efficient hazardous elements adsorption, Sci. Total Environ. 767 (2021), 144973, https://doi.org/10.1016/j.scitotenv.2021.144973.
[70] R. Occhipinti, A.M. Fernandez-Jimenez, A. Palomo, S.C. Tarantino, M. Zema, Sulfate-bearing clay and Pietra Serena sludge: raw materials for the development of alkali activated binders, Constr. Build. Mater. 301 (2021), 124030, https://doi.org/10.1016/j.conbuildmat.2021.124030.
[71] S. Chen, Y. Zhang, D. Yan, J. Jin, Y. Tian, Y. Liu, X. Qian, Y. Peng, S. Fujitsu, The influence of Si/Al ratio on sulfate durability of metakaolin-based geopolymer, Constr. Build. Mater. 265 (2020), 120735, https://doi.org/10.1016/j.conbuildmat.2020.120735.
[72] P. Krivenko, V. Kyrychok, Advances in geopolymer-zeolite composites – synthesis and characterization: Monograph, in: P. Vizureanu, P. Krivenko (Eds.), IntechOpen, London, 2021. https://doi.org/10.5772/intechopen.93360.
[73] X.R.W. Pang, J. Yu, Q. Huo, J. Chen, Chemistry of Zeolites and Related Porous Materials: Synthesis and Structure, John Wiley & Sons (Asia) Pte Ltd., 2007.
[74] P.V. Krivenko, R.V. Runova, M.A. Sanitsky, I.I. Rudenko, Alkali-activated cements: monography, Osnova LTD, 2015.
[75] A.M. Akimkhan, Structural and Ion-Exchange Properties of Natural Zeolite, in Ion Exchange Technologies, ed. by Ayben Kilislioğlu, IntechOpen, 2012. https://doi.org/10.5772/51682.
[76] M.M.J. Treacy, J.B. Higgins, Collection of Simulated XRD Powder Patterns for Zeolites, 5th ed., Elsevier, 2007. https://doi.org/10.1016/B978-0-444-53067-7.X5470-7.
[77] J.E.F.M. Ibrahim, et al., Synthesis and characterization of alkali-activated zeolite-poor rocks, J. Phys. Conf. Ser. 2315 (2022), 012020, https://doi.org/10.1088/1742-6596/2315/1/012020.
[78] D. Novembre, D. Gimeno, M. Calista, V. Mancinelli, F. Miccadei, On the suitability of phillipsite-chabazite zeolitite rock for ammonia uptake in water: a case study from the Pescara River (Italy), Sci. Rep. 12 (1) (2022) 9284, https://doi.org/s41598-022-13367-y.
[79] M. Sakızcı, Investigation of thermal and structural properties of natural and ion-exchanged analcime, Anadolu University J. Sci. Technol. A – Appl. Sci. Eng. 17 (2016) 724–734, https://doi.org/10.18038/aubtda.266863.
[80] P. Dariz, J. Neubauer, F. Goetz-Neunhoeffer, T. Schmid, Calcium aluminates in clinker remnants as marker phases for various types of 19th-century cement studied by Raman microspectroscopy, Eur. J. Mineral. 28 (5) (2016) 907–914, https://doi.org/10.1127/ejm/2016/0028-2577.
[81] K. Arbi, A. Palomo, A. Fernández-Jiménez, Alkali-activated blends of calcium aluminate cement and slag/diatomite, Ceram. Int. 39 (8) (2013) 9237–9245, https://doi.org/10.1016/j.ceramint.2013.05.031.
[82] J. Provis, Geopolymers and other alkali activated materials: why, how, and what? Mater. Struct. 47 (2014) 11–25, https://doi.org/10.1617/s11527-013-0211-5.
[83] T. Kostyuk, V. Vinnichenko, A. Plugin, O. Borziak, A. Iefimenko, Physicochemical studies of the structure of energy-saving compositions based on slags, IOP Conf. Ser. Mater. Sci. Eng. 1021 (1) (2021), 012016, https://doi.org/10.1088/1757-899X/1021/1/012016.
[84] J.L. Provis, S.A. Bernal, Geopolymers and related alkali-activated materials, Annu. Rev. Mater. Res. 44 (2014) 299–327, https://doi.org/10.1146/annurev-matsci-070813-113515.
[85] A. Vollpracht, B. Lothenbach, R. Snellings, et al., The pore solution of blended cements: a review, Mater. Struct. 49 (2016) (2016) 3341–3367, https://doi.org/10.1617/s11527-015-0724-1.
[86] V. Kyrychok, P. Kryvenko, S. Guzii, Influence of the cao-containing modifiers on the properties of alkaline alyumosilicate binders, Eastern-Eur. J. Enterprise Technol. 2 (6–98) (2019) 36–42. https://doi.org/10.15587/1729-4061.2019.161758.
[87] Ch. Baerlocher, L.B. McCusker, D.H. Olson, Atlas of Zeolite Framework Types, 6th ed., Elsevier, 2007.
[88] A. Philip, P.E. Schweitzer, Paint and Coatings: Applications and Corrosion Resistance, Taylor & Francis, New York, 2006.